Temperature range of superconducting fluctuations above Tc in YBa2Cu3O7−δ single crystals

Grbić, Mihael Srđan; Požek, Miroslav; Paar, Dalibor; Hinkov, Vladimir; Raichle, Markus; Haug, Daniel; Keimer, Bernd; Barišić, Neven; Dulčić, Antonije

Source / Izvornik: **Physical review B: Condensed matter and materials physics, 2011, 83**

Journal article, Published version
Rad u časopisu, Objavljena verzija rada (izdavačev PDF)

https://doi.org/10.1103/PhysRevB.83.144508

Permanent link / Trajna poveznica: https://urn.nsk.hr/urn:nbn:hr:217:371162

Temperature range of superconducting fluctuations above T_c in $YBa_2Cu_3O_{7-\delta}$ single crystals

M. S. Grbić,[1] M. Požek,[1] D. Paar,[1] V. Hinkov,[2] M. Raichle,[2] D. Haug,[2] B. Keimer,[2] N. Barišić,[3] and A. Dulčić[1,*]

[1]*Department of Physics, Faculty of Science, University of Zagreb, PO Box 331, HR-10002 Zagreb, Croatia*

[2]*Max-Planck-Institut für Festkörperforschung, D-70569 Stuttgart, Germany*

[3]*1. Physikalisches Institut, Universität Stuttgart, D-70550 Stuttgart, Germany*

(Received 27 May 2010; revised manuscript received 15 February 2011; published 13 April 2011)

Microwave absorption measurements in magnetic fields from 0 up to 16 T were used to determine the temperature range of superconducting fluctuations above the superconducting critical temperature T_c in $YBa_2Cu_3O_{7-\delta}$. Measurements were performed on deeply underdoped, slightly underdoped, and overdoped single crystals. The temperature range of the superconducting fluctuations above T_c is determined by an experimental method which is free from arbitrary assumptions about subtracting the nonsuperconducting contributions to the total measured signal and/or theoretical models to extract the unknown parameters. The superconducting fluctuations are detected in the ab plane, and c-axis conductivity, by identifying the onset temperature T'. Within the sensitivity of the method, this fluctuation regime is found only within a fairly narrow region above T_c. Its width increases from 7 K in the overdoped sample ($T_c = 89$ K) to, at most, 23 K in the deeply underdoped sample ($T_c = 57$ K), so that T' falls well below the pseudogap temperature T^*. Implications of these findings are discussed in the context of other experimental probes of superconducting fluctuations in the cuprates.

DOI: 10.1103/PhysRevB.83.144508 PACS number(s): 74.72.−h, 74.25.N−, 74.40.−n, 74.25.Dw

I. INTRODUCTION

Superconducting fluctuations have attracted a great deal of attention in the research of high temperature superconductors (HTSC). The first reason for this was the challenge of observing the critical regime of fluctuations, which had been previously inaccessible in experiments with classical low temperature superconductors. Due to the short coherence lengths and high thermal energy $k_B T_c$, it was estimated from the Ginzburg criterion that critical fluctuations in HTSC could extend within 1 K or more around T_c (Ref. 1). Beyond the critical region, one expected a transition to Gaussian fluctuations, which are the lowest order fluctuation correction to the mean field theory.[2,3] Indeed, critical fluctuations have been observed in HTSC by a number of experimental techniques, including penetration depth measurements,[4] thermal expansivity[5,6], two-coil inductive measurements,[7] and microwave measurements.[8–12] The experimental evidence was consistent with the three-dimensional (3D) XY universality class. The 3D character implies that the fluctuation correlations extend over many atomic layers along the c axis. Even in strongly underdoped $YBa_2Cu_3O_{7-\delta}$ (YBCO), which is extremely anisotropic, no evidence was found for the crossover to uncorrelated fluctuations in adjacent layers (i.e., the Kosterlitz-Thouless-Berezinsky (KTB) vortex-unbinding transition[13]) until the thickness of the sample became comparable to the fluctuation correlation length.[14]

The second reason for the study of superconducting fluctuations in HTSC was related to the nature of the pseudogap, which is known to open in underdoped compounds at a temperature T^*, much above the superconducting transition temperature T_c (Ref. 15). The intriguing question was whether a highly sensitive experimental technique could detect the superconducting fluctuations extending as high above T_c to almost reach the pseudogap temperature T^*. Observation of the superconducting fluctuations up to T^* would indicate that the pseudogap is related to superconductivity. In such a scenario, the long-range coherence is lost at T_c due to fluctuations of the phase of the superconducting order parameter.[16–21] The pseudogap region would then be marked by preformed Cooper pairs and take the role of the precursor to the superconducting state. If, in contrast, one finds convincing experimental evidence that the onset temperature of the superconducting fluctuations falls well below T^*, in particular, for underdoped HTSC, the nature of the pseudogap would appear to be unrelated to superconductivity. Instead, it could be explained by fluctuations of other order parameters, as proposed on theoretical grounds.[22–24]

Experiments probing magnetic correlations have recently uncovered evidence of electronic liquid-crystal states[25–27] and/or orbital-current order[28–31] in the pseudogap regime of underdoped HTSC. The onset of these ordering phenomena was found to coincide with T^*, as determined by the departure from linearity of the dc resistivity curve. However, the evidence presented in favor of new forms of magnetic order in the pseudogap region need not exclude the existence of some form of the superconducting order, or the possible competition of the two.[32] The extent of the superconducting fluctuations has to be firmly established using a sensitive and reliable experimental technique.

A major problem in most experimental techniques is to subtract properly a background signal unrelated to superconductivity. For example, when analyzing the Nernst effect one has to subtract the normal quasiparticle contribution,[33,34] which may not obey the usual assumptions of the so-called Sondheimer cancellation.[35] Furthermore, it has also been shown that spin/charge density modulations, known as stripe order in underdoped HTSC, can cause a considerable contribution to the observed Nernst signal.[36] The conclusions on the extent of the superconducting fluctuations drawn from the Nernst effect measurements are still controversial[37,38] and call for a complementary analysis by other experimental techniques.

Early work on dc fluctuation conductivity in HTSC relied on the assumption that the normal state resistivity was linear, not only at temperatures far above T_c, but also closer to

T_c where the superconducting fluctuations appear.[39–42] The linearly extrapolated resistivity was used to calculate the normal conductivity σ_n, which was then subtracted from the total experimental conductivity to obtain the fluctuation conductivity alone. However, it was later shown that the linear normal state resistivity was not generic to HTSC, particularly not in underdoped compounds,[15,43] so that deviations from linearity could not be unambiguously ascribed to superconductivity.

In microwave measurements one can determine the complex conductivity $\tilde{\sigma} = \sigma_1 - i\sigma_2$ (Refs. 8, 11, 12, and 44), where the real part σ_1 includes both the normal conductivity σ_n and the contribution from the superconducting fluctuations σ_1'. Separating those two parts poses the same problem as in the dc conductivity analysis. The imaginary part σ_2 requires no subtractions since it is entirely due to the appearance of superconductivity. However, it decays above T_c much faster than the real part σ_1' of the fluctuation conductivity,[45] and may become untraceable due to the signal noise. To deal with the problem, we have recently introduced a novel approach to microwave measurements in combination with an external magnetic field.[46] The microwave signal measured in an 8 T field was subtracted from the one in zero field, and the difference was reliably attributed to the contribution of the superconducting fluctuations above T_c. In a nearly optimally doped $HgBa_2CuO_{4+\delta}$ (Hg1201) high-quality single crystal[47] with $T_c = 94.3$ K, we could observe the superconducting fluctuations up to $T' = 105$ K, which is only 10 K above T_c. This is far below the pseudogap temperature $T^* = 185$ K determined in this compound.

In this paper, we take advantage of the microwave technique combined with the magnetic field to study the superconducting fluctuations in YBCO single crystals over a wide doping range. We have studied both overdoped and underdoped samples (Table I). For a short notation, we name these samples OD89, UD87, and UD57. The experimental arrangement allows for the determination of the superconducting fluctuation conductivity separately in the *ab* plane and along the *c* axis. Our results show that the region of superconducting fluctuations is fairly narrow. In the overdoped sample, it extends to only 7 K above T_c, while in our most underdoped sample at most to 23 K, which falls far below the pseudogap at that doping. The implications of these findings will be discussed.

II. EXPERIMENT

High-quality YBCO single crystals were grown by the solution growth method in the crystal growth group at the Max-Planck-Institut für Festkörperforschung Stuttgart. To prepare samples with well-defined oxygen content the as-grown crystals were annealed in O_2 (OD89 and UD87) and synthetic air (UD57), respectively. The overdoped crystal was detwinned by the application of uniaxial mechanical stress ($\sim 5 \times 10^7$ N/m^2) along the crystallographic ⟨100⟩ direction at elevated temperatures. Further details about the sample preparation are given in Ref. 48.

TABLE I. Some physical properties of the measured samples. N_{ab} and N_c are the demagnetization factors (Ref. 49) for H_{mw} parallel to the *ab* plane and the *c* axis, respectively.

Sample	Doping p	T_c(K)	ΔT_c(K)	Size (mm^3)	N_{ab}	N_c
OD89	0.19	89.4	1.6	$2.5 \times 1.9 \times 0.6$	0.13	0.68
UD87	0.15	87.2	2	$2.5 \times 1.95 \times 1$	0.26	0.56
UD57	0.12	57.2	5	$2.5 \times 1.6 \times 0.9$	0.29	0.55

Table I summarizes the main characteristics of the measured samples. The hole doping level per planar Cu ion p was extracted from the known doping dependence of the room-temperature thermoelectric power[50] and the lattice parameter *c* (Ref. 51). The width ΔT_c of the superconducting transition was estimated by the common 10–90% criterion of the transition curve measured by the microwave absorption described later in this paper. We may note that the same criterion applied in dc resistivity curves yields a smaller transition width. This comes out naturally because of the nonzero losses in microwave measurements even below T_c. Thus, the present estimate of ΔT_c is a rather conservative one. The precise value quoted for T_c is not the simple midpoint in the transition curve measured by the microwave absorption, but was inferred from the maximum of the real part σ_1 of the complex microwave conductivity as shown later in Sec. V. This value of T_c was found to lie within the ΔT_c range, somewhat closer to the lower (10%) boundary.

For the microwave measurements, the sample was mounted on one end of a sapphire holder, which serves as a cold finger. The assembly was then inserted into the microwave cavity so that the sample takes the center position inside. Outside of the microwave cavity, a heater-sensor block was mounted on the free end of the sapphire holder. The temperature could be controlled to 10 mK stability. The microwave cavity was made of copper so as to allow measurements in any external magnetic field with only a small change in its Q factor. This small field-dependent variation could be detected by measuring the empty cavity and subtracted from the signal measured when the cavity was loaded with the sample.

The geometry of the microwave cavity was carefully chosen as elliptic so that the degeneracy of some orthogonal modes could be lifted. We used ${}_e\mathrm{TE}_{112}$ and ${}_e\mathrm{TE}_{211}$ modes operating at 13.14 and 15.15 GHz, respectively. Each of these modes has an antinode of the microwave magnetic field H_{mw} in the cavity center, where the sample is positioned. However, the polarization of H_{mw} is along the cavity axis in the ${}_e\mathrm{TE}_{211}$ mode and perpendicular to this axis in the ${}_e\mathrm{TE}_{112}$ mode. Thus, with the same mounting and positioning of the sample in the cavity, we could carry out two measurements. We chose to mount the YBCO single crystal so that its *c* axis was along the cavity axis (vertical in our experimental setup). Consequently, the induced microwave currents in the measurement with the ${}_e\mathrm{TE}_{211}$ mode were flowing as closed loops in the *ab* plane, while the ${}_e\mathrm{TE}_{112}$ yielded microwave currents closing the loops by flowing partly in the *ab* plane and partly along the *c* axis. The polarizations of H_{mw} and the induced current loops in the two respective modes are shown in the insets of Figs. 1 and 2.

The microwave source was a Rohde Schwarz synthesizer whose frequency could be tuned to achieve resonance. An automatic frequency control (AFC) circuit allowed tracking of the resonance as the temperature of the sample was swept, and the resonant frequency was measured by a microwave counter. On top of that, the microwaves were frequency modulated

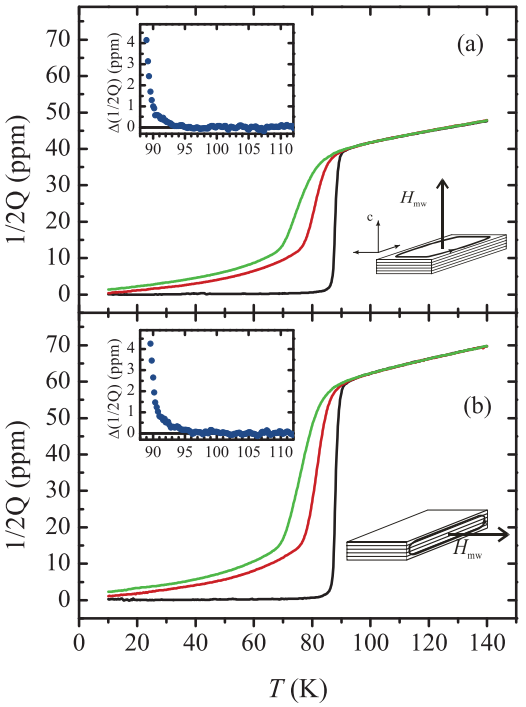

FIG. 1. (Color online) Microwave absorption in slightly underdoped YBCO ($T_c = 87$ K). External dc magnetic field is applied parallel to the c axis (black: $B_{dc} = 0$; red: $B_{dc} = 8$ T; green: $B_{dc} = 16$ T). (a) $H_{\rm mw}$ is in the c direction so that the induced microwave currents flow in the ab plane. (b) $H_{\rm mw}$ lies in the ab plane so that the induced microwave currents flow partly in the c-direction and partly in the ab plane. Insets show the difference in absorption between $B_{dc} = 16$ T and zero field for their respective configurations.

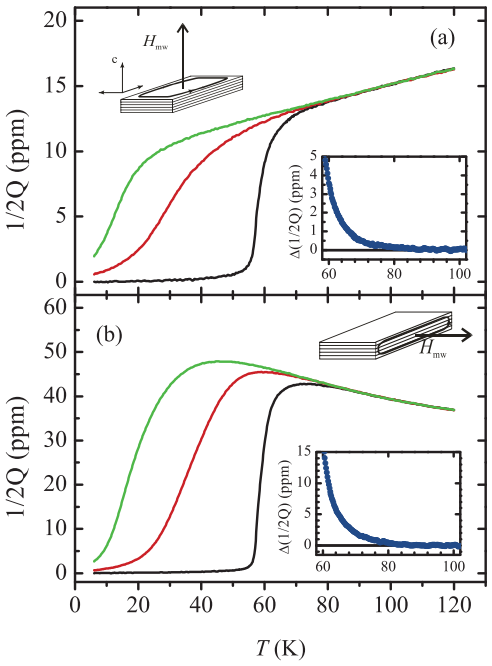

FIG. 2. (Color online) Microwave absorption in deeply underdoped YBCO ($T_c = 57$ K). External dc magnetic field is applied parallel to the c axis (black: $B_{dc} = 0$; red: $B_{dc} = 8$ T; green: $B_{dc} = 16$ T). (a) $H_{\rm mw}$ is in the c direction so that the induced microwave currents flow in the ab plane; (b) $H_{\rm mw}$ lies in the ab plane so that the induced microwave currents flow partly in the c direction and partly in the ab plane. Insets show the difference in absorption between $B_{dc} = 16$ T and zero field for their respective configurations.

at 991 Hz, with a frequency deviation which corresponds to the half-width of the Lorentzian representing the resonance curve of the microwave cavity loaded with the sample. Even harmonics of the output signal from the microwave cavity were used to determine very accurately the Q factor of the cavity. The details of this method were published elsewhere.[52]

Data acquisition was made during a slow temperature sweep of the sample so that the microwave signal generator could alternate between the resonance frequencies of the two modes. Thus, we obtained the experimental curves in both modes with a single temperature sweep. This procedure ensures that the resulting data can be directly compared.

III. MICROWAVE ABSORPTION AND SUPERCONDUCTING FLUCTUATIONS

The results of microwave measurements are expressed through a change in the inverse value of the quality factor of the cavity loaded with the sample. In our experimental setup, the microwave cavity is kept always at a constant low temperature (e.g., 2 K) so that the power dissipation in its walls remains unchanged. The contribution of the unloaded cavity, $1/2Q_0$, is subtracted from the total experimental value $1/2Q_{\rm exp}$ to obtain the contribution due to the sample itself $1/2Q = 1/2Q_{\rm exp} - 1/2Q_0$. As the temperature of the sample is varied, one observes changes of $1/2Q$ as the absorption of microwaves is changed within the skin depth of the sample surface.

A. Slightly underdoped sample

To extract the contribution of the superconducting fluctuations from the overall signal, we have carried out measurements in zero magnetic field and in (dc) magnetic fields up to 16 T. The behavior of the superconducting fluctuations in applied magnetic fields has been previously studied by dc conductivity measurements[53–55] and compared to theoretical predictions.[56] Also, microwave conductivity measurements were used for studying the scaling properties in field and temperature.[57] In contrast to those studies, here we do not aim to study the superconducting fluctuations in various applied fields, but apply a high enough field to suppress superconductivity at all temperatures above the zero field T_c. This serves us to determine the normal state background line without any extrapolation based on a theoretical model of the normal state behavior. In Sec. V we will show more explicitly that the 8 T field is already sufficient for this task and the 16 T field can further suppress the superconductivity a few degrees below the zero field T_c.

Figure 1 shows the curves measured in the slightly underdoped YBCO single crystal in zero magnetic field, as well as in various applied magnetic fields. In an applied magnetic field, the superconducting transition is shifted to a lower temperature and occurs through the formation of the mixed state with some magnetic flux penetrating into the sample.

The microwave currents then exert a Lorentz force on vortices so that their oscillation constitutes an additional mechanism of the microwave power absorption.[58–60]

The measurements shown in Figs. 1(a) and 1(b) were carried out in the two modes as described in Sec. II. Note that the signal in the normal state is considerably larger when $H_{\rm mw}$ is parallel with the ab plane [Fig. 1(b)]. The explanation can be found if one observes that, in this configuration, the induced current flows in a closed loop, partly in the ab plane and partly along the c axis. Since the ratio of the normal state values ρ_c and ρ_{ab} is much larger than the ratio of the sample dimensions (the respective current paths), the main contribution to the absorption signal comes from the current path along the c axis. The detailed analysis of ρ_{ab} and ρ_c in all three samples will be postponed to Sec. IV.

Here we focus on the superconducting fluctuations above T_c. It is evident in Figs. 1(a) and 1(b) that, at higher temperatures, the curves measured in applied fields of 16 and 8 T merge with the curve which was measured when no external magnetic field was applied. This overlap holds even on an expanded scale when the signal noise can be seen directly. It is useful to quantify this statement by analyzing the data in Fig. 1(a). The total signal $1/2Q$ above T_c is in the range 40–50 ppm, whereas our noise level in that temperature range is about 0.2 ppm. Hence, we can positively detect a relative change in our signal which is greater than $(1/2)10^{-2}$. Noting that $1/2Q$ is related to the surface resistance R_s by a constant geometric factor and $R_s \propto \sqrt{\rho}$, one finds that our method can detect a relative change in the resistivity $\Delta\rho/\rho$ greater than 10^{-2}. A typical value for slightly underdoped YBCO at 100 K is about 100 $\mu\Omega$cm (Ref. 61) so that our method is sensitive to resistivity changes greater than 1 $\mu\Omega$cm. Within this limit, we observe no magnetoresistance in fields up to 16 T in the normal state above 100 K in nearly optimally doped YBCO. We note, however, that the transverse and longitudinal dc magnetoresistance of magnitude $\sim 10^{-6}$ has been observed up to $\sim$270 K over a wide range of underdoped YBCO (Ref. 62). The small longitudinal magnetoresistance at high temperatures was ascribed to magnetic scattering which increases when the spin gap is suppressed by the Zeeman effect, while a much larger magnetoresistance closer to T_c was ascribed to the superconducting fluctuations. Orbital magnetoconductivity in the normal state at higher temperatures was fitted very well with the $(aT^2 + b)^{-2}$ dependence, while an upturn from this behavior was observed only when it reached the magnitude $\sim 10^{-4}$ at temperatures about 20 K above T_c.

We conclude that the difference of the zero field and 16 T curves in Fig. 1(a) can be used to analyze the appearance of the superconducting fluctuations above T_c. It is shown in the inset of Fig. 1(a) on an expanded scale. The noise signal of about 0.2 ppm is clearly seen. The deviation from zero can be estimated to occur below 95 K. Below this temperature the superconducting fluctuations appear and give rise to an excess conductivity. In the ac case, the superconducting conductivity is complex, but the onset of fluctuations is dominated by the real part of this conductivity. Here we can state that the superconducting fluctuations extend from $T_c = 87$ K to $T' = 95$ K (i.e., in the range of only 8 K) as seen from the insets in Figs. 1(a) and 1(b). It is important to note that similar results were found in nearly optimally doped Hg1201 single crystals[46] and $La_{2-x}Sr_xCuO_4$ (LSCO) (Ref. 63), indicating that this feature might be universal for nearly optimally doped HTSC.

B. Deeply underdoped sample

The microwave results in the deeply underdoped YBCO sample UD57 are shown in Fig. 2. In the configuration where the microwave currents flow solely in the ab plane [Fig. 2(a)], one observes, even at such a low doping level, metallic behavior in the normal state around 100 K, similarly as in the nearly optimally doped sample above. This is consistent with dc measurements of ρ_{ab} in a series of YBCO samples.[61]

The transition to the superconducting state in Fig. 2(a) is shifted to lower temperatures and greatly broadened with respect to the slightly underdoped sample [compare Fig. 1(a)]. The difference of the zero field and 16 T curves is shown in the inset of Fig. 2(a) on an expanded scale. Some contribution of superconductivity is seen up to 80 K (i.e., 23 K above T_c). A similar temperature range of superconducting fluctuations in transport measurements was already reported for other HTSC materials [e.g., in underdoped samples of $Bi_2Sr_2CaCu_2O_8$ (Bi2212), Ref. 44 and Co-substituted YBCO, Ref. 64]. However, we should also consider the possibility that the sample might not be perfectly homogeneous, in which case some fractions of the sample would have T_c values distributed slightly above 57 K and reaching even 80 K. In this scenario, the superconducting fluctuations due to the main body of the sample might extend from 57 K to some temperature below 80 K, with their contribution to the superconducting conductivity being masked by that of a small-volume fraction of the sample having a distribution of T_c values in that same temperature range. This, however, seems to be a minor effect in the freshly prepared sample. We demonstrate in Fig. 3 that the microwave absorption can sensitively detect when a significant distribution of T_c is introduced in the same sample after an extended period of aging (nearly five years in a closed box). Similar observations were reported earlier in fluctuation diamagnetism of two YBCO samples (chain ordered and chain disordered) of the same T_c (Ref. 65). Our results for the extent of the superconducting fluctuations are consistent with those of Ref. 66 (Nernst effect) for a sample with the same T_c before introducing disorder and the result of Ref. 67 (Hall effect). Within the sensitivity of our method, we can conclude that the observed superconducting fluctuations extend at maximum 23 K above T_c in our UD57 YBCO sample.

The experimental curves presented in Fig. 2(b) for the configuration in which $H_{\rm mw}$ lies in the ab plane exhibit a different behavior than those in the nearly optimally doped sample [cf. Fig. 1(b)]. The semiconducting behavior in the normal state is obviously due to the contribution of the current flowing along the c axis [inset in Fig. 2(b)]. The detailed behavior of ρ_{ab} and ρ_c is given later in Sec. IV.

The application of a high external magnetic field acts to suppress superconductivity close to T_c so that the semiconductor-like behavior in Fig. 2(b) is extended to lower temperatures. The difference in the signals measured in the 16 T and zero field is shown in the inset to Fig. 2(b) on an expanded scale.

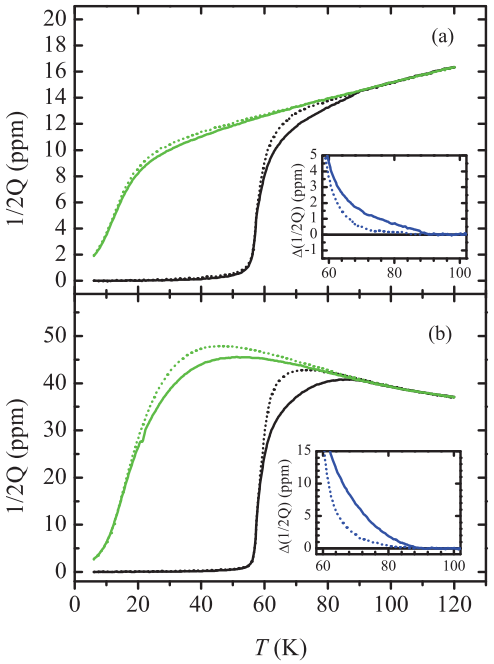

FIG. 3. (Color online) Microwave absorption in the deeply underdoped UD57 YBCO sample before (dotted lines) and after aging at room temperature in air (solid lines). The latter data show that the intake of oxygen takes place during aging and a small fraction of the sample becomes optimally doped. External dc magnetic field is applied parallel to the c axis (black: $B_{dc} = 0$; green: $B_{dc} = 16\,\mathrm{T}$). (a) H_{mw} is in the c direction so that the induced microwave currents flow in the ab plane; (b) H_{mw} lies in the ab plane so that the induced microwave currents flow partly in the c direction and partly in the ab plane. Insets show the difference in absorption between $B_{dc} = 16\,\mathrm{T}$ and zero field for their respective configurations.

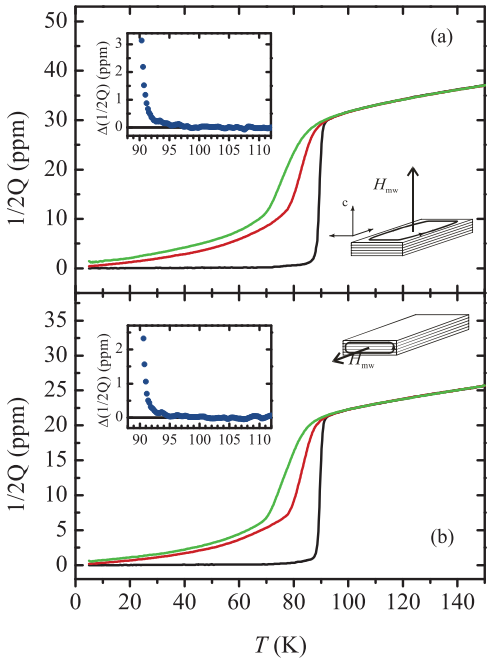

FIG. 4. (Color online) Microwave absorption in overdoped YBCO ($T_c = 89\,\mathrm{K}$). External dc magnetic field is applied parallel to the c axis (black: $B_{dc} = 0$; red: $B_{dc} = 8\,\mathrm{T}$; green: $B_{dc} = 16\,\mathrm{T}$). (a) H_{mw} is in the c direction so that the induced microwave currents flow in the ab plane; (b) H_{mw} is parallel to the a axis so that the induced microwave currents flow partly along the c axis and partly along the b axis. Insets show the difference in absorption between $B_{dc} = 16\,\mathrm{T}$ and zero field for their respective configurations.

Again we find that the upper limit of the appearance of superconducting fluctuations is set at 80 K.

C. Overdoped sample

We now turn to the overdoped side of the YBCO phase diagram. The measurements of the OD89 sample are shown in Fig. 4. At this doping level the crystal structure is fully oxygenated, which enhances the interlayer coupling and results in a coherent normal-state transport along the c axis.[68,69] The resistivity ρ_c is greatly reduced with respect to the underdoped samples and the anisotropy ρ_c/ρ_{ab} becomes small. As a result, the relative contribution of ρ_c to the signal in Fig. 4(b) is less pronounced than in the corresponding measurements of the underdoped samples. In Sec. V, we show that it was still possible to separately extract ρ_{ab} and ρ_c in the overdoped sample. Here we analyze the raw data curves by the same procedure as in the underdoped samples above. The difference of the zero field and 16 T curves shows that even in the overdoped sample the superconducting fluctuations are visible up to $T' = 96\,\mathrm{K}$ (i.e., 7 K above T_c).

D. Interpretation of the experimental data in the fluctuation regime

Given the controversy that persists in the current literature about the temperature range of the superconducting fluctuations above T_c in HTSC, we find it important to interpret our raw experimental data before performing any analysis which involves theoretical models and/or assumptions on unknown behavior in the normal state. Our measurements of microwave absorption in progressively higher applied magnetic fields have shown that an 8 T field is already sufficient to suppress superconductivity at temperatures above the zero-field T_{c0} (cf. Fig. 6 in Sec. V). Here we use the curves measured in a 16 T field to represent the normal state at all temperatures above the zero-field T_{c0} and observe the difference between these curves and those measured in the zero applied field. Our results show that superconducting fluctuations extend 7–8 K above the zero-field T_{c0} in overdoped and slightly underdoped YBCO samples, while in deeply underdoped YBCO sample the superconducting fluctuations extend at most up to 23 K above the zero-field T_{c0}. The latter result is the most intriguing in the current controversy about the nature of the pseudogap in deeply underdoped HTSC.

According to the theoretical analysis made by Emery and Kivelson,[16,17] the superconducting order parameter in underdoped HTSC samples has a low phase stiffness (superfluid density of the system ρ_s), so that long-range phase coherence can be achieved only below some temperature T_θ, which is lower than the mean field transition temperature T^{MF}. The temperature T_θ then plays the role of the superconducting transition T_c which, in a real system, may be additionally lowered by the effects of some other degrees of freedom. Thus, above T_c this theory predicts the predominance of phase fluctuations extending in a wide temperature region. Some of

the previous experimental observations may have observed this behavior.[44,46,66] Furthermore, this theory predicts that even above the phase fluctuation region, and up to T^{MF}, one may have uncorrelated Cooper pairs (i.e., those which are not capable of forming even short-range and short-lived phase coherence.[70]) The crucial question is how high above T_c can the superconducting fluctuations survive and what experimental techniques can be used to positively detect them.

An external magnetic field perturbs the phase and amplitude of the superconducting order parameter. Which of the two components will be affected in the first line depends on the phase stiffness of the system. The present experiments detect superconducting fluctuations which appear with some amplitude and phase correlation. In this sense, they are analogous to Josephson tunneling experiments reported previously.[64] It is interesting to compare the frequency range of the detected fluctuations. Our experiments probe the superconducting fluctuations in the GHz frequency range and we have shown that these fluctuations extend up to at most 23 K above T_c for the UD57 sample. The excess conductance measured in the Josephson tunneling experiment as a function of the applied voltage revealed the superconducting fluctuations up to 1 THz frequency range at temperatures 14 K above T_c in a Co-substituted YBCO sample with a similar doping level.[64] These are conventional amplitude and phase superconducting fluctuations which are shown to persist within a relatively narrow temperature interval above T_c.

However, it is worth mentioning here that the measurements of the far-infrared (FIR) optical conductivity can probe the electron system at much higher frequencies.[71] By considering the temperature dependence of the optical spectral weight, a recent FIR study in deeply underdoped YBCO (similar to our UD57 sample) has uncovered possible evidence for superconducting fluctuations up to temperatures as high as 180 K (Ref. 72). The result was obtained using a multilayer model of the *c*-axis electrodynamics, which separates the local intrabilayer and interbilayer conductivity in YBCO. Only the intrabilayer conductivity was found to develop precursor conductivity at elevated temperatures. It gives rise to a transverse plasma mode and anomalous temperature dependence of some infrared-active phonon modes. One may recall that neutron scattering experiments on underdoped YBCO have revealed spin correlations well above T_c with fluctuation rates in the THz range.[25,26] These spin correlations also develop a characteristic in-plane anisotropy, which has been interpreted in terms of an electronic transition into a nematic liquid state. This process may be related to the intrabilayer anomalies observed in FIR measurements.

On the other hand, microwave *c*-axis conductivity can detect superconductor (SC) fluctuations capable of forming long-range interbilayer correlations. This can be further confirmed by comparing the samples with higher doping levels, where the correlations extend in the same temperature range when detected by both microwave and FIR techniques. Namely, for the optimally doped and overdoped cuprates, model calculations[16,73] show that the phase stiffness is more rigid ($T_\theta > T^{MF}$), so that the transition to the normal state is expected to occur through the disappearance of the amplitude of the order parameter. Hence, above T_c the superconducting fluctuations would preserve phase correlation as long as there is some amplitude present (i.e., amplitude fluctuations alone cannot be expected on theoretical grounds). The present measurements in our slightly underdoped (UD87) and overdoped (OD89) samples have detected the superconducting fluctuations in the range of 7–8 K above T_c, which is a considerably shorter range than the one observed in the deeply underdoped (UD57) sample, but does not reduce to the narrow-range characteristic of classical superconductors. These observations are similar to the ones noted in recent measurements of the Nernst coefficient in YBCO single crystals at different magnetic fields.[38] Also, dynamic scaling analysis of the microwave conductivity in LSCO samples with a broad range of doping has shown a narrow range of fluctuations above T_c (Ref. 74). The same conclusion about the narrow range of fluctuations above T_c has been recently drawn from THz time-domain spectroscopy in LSCO thin films with a doping range that spans almost the entire superconducting dome.[75]

IV. ANISOTROPIC RESISTIVITIES

Having established the extent of the superconducting fluctuations above T_c directly from the measured data, we can proceed with a theoretical analysis of the measured curves and reach additional conclusions which go beyond those of direct observation.

In the course of microwave measurements, one determines two parameters, $1/2Q$ and $\Delta f/f$, where Δf is the shift of the resonant frequency at a given temperature with respect to the lowest temperature value. The two parameters are combined to

$$\frac{1}{2Q} - i\frac{\Delta f}{f} = \Gamma(R_s + i\Delta X_s), \tag{1}$$

where Γ is a geometric factor for a given sample in the cavity, which is not changed upon temperature variation (i.e., it holds for the entire set of data). It can be calculated if the resistivity ρ_n is known at some temperature well above T_c so that the sample is fully in the normal state. The calculated value of the normal surface resistance $R_{sn} = \sqrt{\omega\mu_0\rho_n/2}$ is then simply compared to the measured value of $1/2Q$ at that temperature.

One has to set an offset value to the measured frequency shift in Eq. (1) so that the full value of the surface reactance X_s also appears in that equation. This can be accomplished through knowledge of the low temperature London penetration depth λ_L, from which one calculates $X_s(0) = \omega\mu_0\lambda_L$, or by assuming that the conductivity in the normal state is a real quantity σ_n so that $X_{sn} = R_{sn} = \sqrt{\omega\mu_0\rho_n/2}$. We adopt the latter procedure for the analysis of our data in YBCO samples. The measured complex frequency shift can then be expressed through the surface impedance $\tilde{Z}_s = R_s + iX_s$ at all temperatures.

The real part of the resistivities ρ_{ab} for the three YBCO samples are shown in Fig. 5(a). They were inferred from the measurements shown in Figs. 1(a), 2(a), and 4(a) where the sample orientation and the selected microwave mode ensured that the current was flowing only in the *ab* plane. The in-plane resistivities are metallic-like, even in the deeply underdoped sample, as has been previously found by dc resistivity measurements.[61]

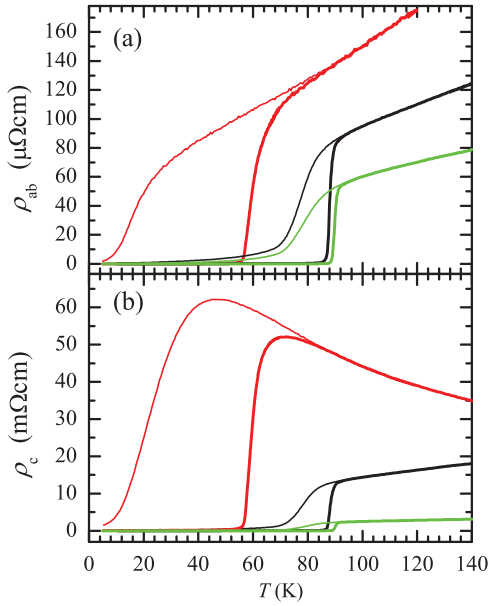

FIG. 5. (Color online) (a) The real part of the *ab*-plane resistivity of the three YBCO samples, OD89 (green), UD87 (black), and UD57 (red) as determined from the microwave measurements in the mode in which the current flows only in the *ab* plane [Figs. 1(a), 2(a), and 4(a)]. Metallic behavior is observed in overdoped and underdoped samples in the normal state. The thicker and thinner lines pertain to the results obtained in zero field and 16 T fields, respectively. (b) The real part of the *c*-axis resistivity determined by the decomposition of the total signal measured in the mode where the current flows partly in the *ab* plane and partly along the *c* axis as shown in the insets of Figs. 1(b), 2(b), and 4(b). The decomposition procedure is described in the text.

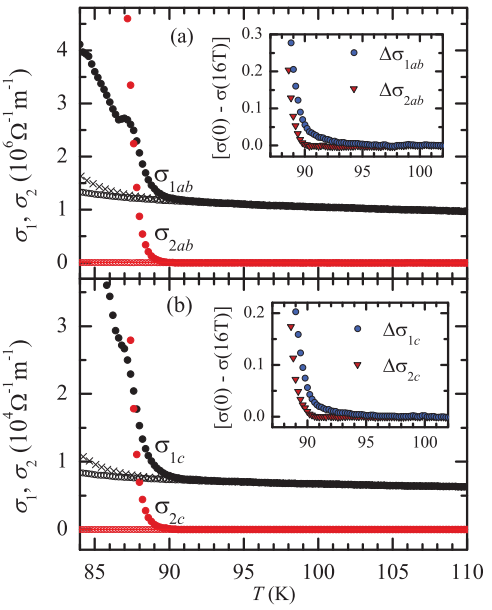

FIG. 6. (Color online) (a) *ab*-plane complex conductivity of the UD87 sample. The data points of the real part of the conductivity (σ_{1ab}) are represented by black symbols while red symbols are used for the imaginary part (σ_{2ab}). Full circles, crosses, and open triangles stand for the conductivities in zero magnetic field, 8 and 16 T fields, respectively. The inset in (a) shows on an expanded scale the difference between the conductivities in zero field and in the field of 16 T ($\Delta\sigma_{1ab}$ blue circles, $\Delta\sigma_{2ab}$ red triangles) at temperatures above the zero-field T_{c0}. (b) The complex conductivity along the *c* axis in the UD87 sample. The presentation is analogous to that of (a).

The resistivity ρ_c can be extracted from the curves shown in Figs. 1(b), 2(b), and 4(b) which are taken in the mode where the current flows partly in the *ab* plane, and partly along the *c* axis. For the microwave field along the *b* axis, the effective measured surface impedance is

$$Z_{\text{eff}} = \frac{abZ_{ab} + bcZ_c}{ab + bc}, \tag{2}$$

where Z_{ab} and Z_c are the true surface impedances depending on the resistivities ρ_{ab} and ρ_c, respectively. The parameters *a*, *b*, and *c* stand for the sample dimensions as given in Table I. The resulting curves for the real part of ρ_c are shown in Fig. 5(b). The slopes of ρ_c in overdoped and slightly underdoped samples exhibit a metallic-like behavior, consistent with previously reported measurements of ρ_c in optimally doped YBCO (Refs. 74 and 76). In deeply underdoped UD57 sample, ρ_c shows a semiconductor-like behavior as previously reported by dc resistivity[43] and microwave measurements[77] in underdoped YBCO. We note here that a similar semiconductor-like behavior of ρ_c has been observed also in nearly optimally doped Hg1201 single crystals below the pseudogap temperature T^* (Ref. 46). However, the Hg1201 system is highly anisotropic already at optimal doping, while the YBCO system acquires a high anisotropy only when deeply underdoped.

V. ANALYSIS OF THE COMPLEX CONDUCTIVITY DUE TO SUPERCONDUCTING FLUCTUATIONS

It is convenient to study the superconducting fluctuations through the complex conductivity $\tilde{\sigma} = \sigma_1 - i\sigma_2$, which can be inferred from the complex surface impedance $\tilde{Z}_s$ using the expression

$$\sigma_1 - i\sigma_2 = \frac{i\omega\mu_0}{Z_s^2}. \tag{3}$$

The resulting real and imaginary parts of the zero field *ab*-plane conductivity in the slightly underdoped UD87 sample are shown in Fig. 6(a). In ac measurements, the superconducting fluctuations bring about finite contribution to conductivities at T_c (Refs. 78 and 79). Moreover, the real part σ_1 has a peak, which may be superimposed on a broader maximum extending below T_c (Refs. 8, 11–13, and 44). The peak in σ_1 is a very useful feature since the zero field T_c can be determined from a physically meaningful observation, rather than by referring to some arbitrary criteria, such as the midpoint on the measured transition curve in Fig. 1(a).

Also shown in Fig. 6(a) are the σ_{1ab} conductivities obtained from the curves measured in the applied magnetic fields of 8 and 16 T. It is evident that the latter two curves overlap at all temperatures above the zero field T_c. In other words, it is sufficient to apply the field of 8 T to suppress all superconductivity above the zero field T_c, and the field of 1616 T is seen to suppress the superconductivity of a few degrees further below the zero field T_c. Hence, by taking

the difference of the conductivities in the zero field and in 16 T field, one may construct a reliable procedure for extracting the pure superconducting fluctuation contribution to the conductivity above the zero field T_c. The inset in Fig. 6(a) shows the result on an expanded scale. It is seen to merge into the signal noise at 95 K. This is the temperature T' that has already been identified directly form the microwave absorption data in Sec. III.

The imaginary part of the fluctuation conductivity σ_{2ab} is also presented in Fig. 6(a). Note that the curves obtained from the measurements in 8 and in 16 T fields are indistinguishable in the whole temperature interval presented in Fig. 6(a). They show zero values, as expected for the imaginary part of the conductivity in the normal state. Hence, the values of σ_{2ab} obtained in the zero field are due to the superconducting fluctuations. These data points are also shown in the inset of Fig. 6(a) on an expanded scale. The imaginary part σ_{2ab} is seen to decay much faster than the real part σ_{1ab}, which is expected at our operating microwave frequency.[45]

Figure 6(b) shows the complex conductivity along the c axis in the UD87 sample. The presentation is analogous to that of the in-plane conductivity in Fig. 6(a). The signature of T_c is visible as a shoulder on the curve of σ_{1c}. We note that both curves, σ_{1ab} and σ_{1c}, yield the same value of T_c. It is the temperature at which the coherence lengths ξ_{ab} and ξ_c diverge. The applied field of 8 T is seen to suppress the superconductivity along the c axis at all temperatures above T_c, similarly as it has been shown in the ab plane. Therefore, the curves measured in the field of 16 T can be safely used to represent the normal state at all temperatures above the zero-field T_c. In the inset of Fig. 6(b) one can observe that the fluctuation contribution to σ_{1c} extends up to 95 K, the temperature also identified as T' in Sec. III.

We have conducted a similar analysis in our deeply underdoped UD57 and overdoped OD89 samples. The general features are common to all three samples. We find that the peak in the real part σ_1 of the complex conductivity, both in the ab plane and along the c axis, can be used to determine the zero-field T_c in each of the samples. Also, the applied field of 16 T is found to be more than sufficient to suppress superconducting fluctuations above T_{c0}, so that the excess fluctuation conductivity above T_c in the zero field can be determined by the above described procedure. It appears that the temperature T', up to which the real part σ_1 of the fluctuation conductivity extends before merging with the noise signal, coincides with the values already established in Sec. III.

It is useful to pay additional attention to the features of the real and imaginary component of the ac conductivity which arise due to the superconducting fluctuations. The data points for the in-plane superconducting fluctuation conductivity above T_c in our slightly underdoped UD87 sample are presented in Fig. 7 against the reduced temperature $t = \ln(T/T_c)$ in a log-log plot. One may try to compare those experimental results to the theoretical predictions for the fluctuation conductivity in anisotropic 3D systems. The test is severe since a single set of parameters is expected to describe well both the real and imaginary components of the fluctuation conductivity.

The frequency-dependent conductivity can be calculated within the Kubo formalism from the current due to the

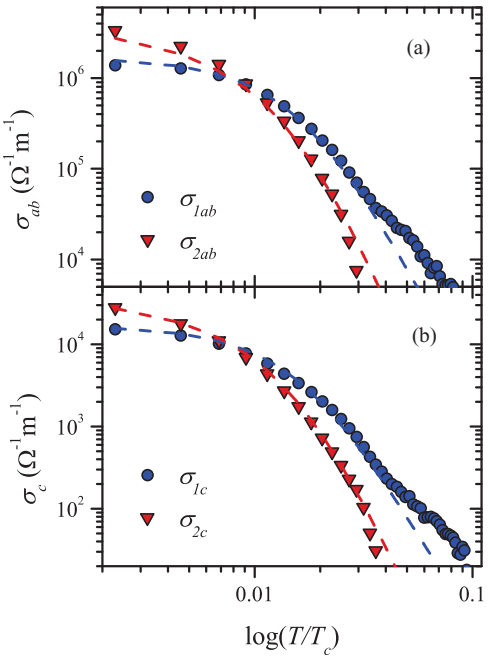

FIG. 7. (Color online) Presentation of the real and imaginary parts of the complex superconducting fluctuation conductivity above T_c as a function of reduced temperature $t = \ln(T/T_c)$ on a log-log plot. Data for the slightly underdoped sample UD87 is shown by full symbols and the dashed lines are theoretical curves as described in the text. (a) In-plane conductivity σ_{1ab} and σ_{2ab}. (b) Conductivity along the c axis σ_{1c} and σ_{2c}.

fluctuations of the order parameter[3,78] or, alternatively, as the response of the system to an external field[79,80]. It was also shown that, for physical reasons, one had to truncate the summation over the fluctuation modes at a minimum wavelength of $2\pi\xi_0/\Lambda$, where ξ_0 is the intrinsic coherence length and Λ is the cutoff parameter.[81,82] Indeed, with no cutoff taken in the calculations, the theoretical dc fluctuation conductivity greatly overestimates the experimentally observed values at temperatures above T_c (Ref. 40). For the in-plane complex ac fluctuation conductivity in anisotropic 3D systems, one obtains[45,83,84]

$$\tilde{\sigma}_{ab} = \frac{e^2}{32\hbar\xi_{c0}}\left(\frac{\xi_{ab}(T)}{\xi_{ab0}}\right)^{z-1}\left[S_1(\omega,T,\Lambda) - iS_2(\omega,T,\Lambda)\right], \tag{4}$$

where the intrinsic coherence length ξ_{c0} along the c axis enters in the prefactor. Here, the time-dependent Ginzburg-Landau theory is used with the relaxational dynamics implying that the dynamical critical exponent $z = 2$. This value of z was found previously by other experimental groups[7,74] and elaborated on theoretical grounds.[85] However, alternative values for the dynamical critical exponent have also been quoted in the literature.[9,10] Recently, it has been shown that the original experimental results in thin films can be analyzed properly only by accounting for the finite size effects and the value of z then extracted.[86] In microwave measurements, the phase of the complex fluctuation conductivity at T_c is often taken as a sensitive probe for the value of z. However, the extracted value of z may still be incorrect if the effect of the short wavelength

cutoff at T_c is not accounted for properly.[45] For those reasons, we retain the relaxational dynamics (model A) with $z = 2$ and determine the cutoff parameter from the fit to the experimental data.

The temperature dependence is expressed through the reduced coherence length $\xi_{ab}(T)/\xi_{ab0}$ in both the prefactor and in the $S_{1,2}$ functions as given explicitly elsewhere.[45,83] Well above T_c one expects the Gaussian regime with $[\xi_{ab}(t)/\xi_{ab0}] = t^{-\nu}$, where $t = (T - T_c)/T_c$ is the reduced temperature, and the static critical exponent $\nu = 1/2$. However, in the critical region close to T_c, the Gaussian regime no longer holds, and one may include the quartic term in the Ginzburg-Landau functional using the Hartree approximation yielding finally a renormalized coherence length[79,87]

$$\frac{\xi_{ab}(T)}{\xi_{ab0}} = \frac{\Gamma}{\ln(T/T_c)}\left(1 + \sqrt{1 + \frac{\ln(T/T_c)}{\Gamma^2}}\right), \qquad (5)$$

where Γ is a parameter which determines the crossover from the Gaussian temperature dependence ($\nu = 1/2$) to the critical regime ($\nu = 1$) close to T_c. Here, T_c is the renormalized critical temperature, as observed in the actual experiment.

The fluctuation conductivity along the c axis takes also the form of Eq. (4), except that ξ_{c0}^{-1} in the prefactor is replaced by $\xi_{c0}/\xi_{ab0}^2 = 1/\gamma^2\xi_{c0}$, where $\gamma = \xi_{ab0}/\xi_{c0}$ is the anisotropy factor.[83] The renormalized coherence length $\xi_c(T)/\xi_{c0}$ should be equal to $\xi_{ab}(T)/\xi_{ab0}$ given in Eq. (5) if the anisotropy does not change with temperature.

Figure 7 shows the calculated ac fluctuation conductivity at our operating frequency of 15.15 GHz. We note first that T_c is determined unambiguously from the peak in σ_1 shown in Fig. 6, hence it is not a free parameter for the fit. This is a salient convenience in the microwave method, as compared to dc conductivity analysis where T_c has to be considered as a fit parameter. Also, ξ_{c0} in Eq. (4) can be determined by evaluating. σ_{2ab} at T_c and equating the result to the experimental value[12,45] In the case of our UD87 sample, we have obtained $\xi_{c0} = 0.08$ nm. The only free parameters are the cutoff parameter Λ in Eq. (4), together with the crossover parameter Γ in Eq. (5). The best agreement of the theoretical curves and the experimental data for σ_{ab} in Fig. 7(a) is obtained with $\Lambda = 0.032$ and $\Gamma = 0.19$. The fit is also very good for σ_c in Fig. 7(b) with the same values of the crossover parameter Γ and the cutoff parameter Λ. The anisotropy parameter was found to be $\gamma = 10$.

A similar analysis of the fluctuation conductivity in our UD57 sample is presented in Fig. 8. Again, T_c is determined from the peak in σ_1 and is not a free parameter in the theoretical calculations. The crossover parameter is free, but we required it to be the same for in-plane and c-axis conductivities. The obtained value $\Gamma = 0.4$ is larger than that found in the slightly underdoped sample UD87, which means that the critical fluctuations have a relatively larger extent in the deeply underdoped sample UD57. The cutoff parameters are different for the in-plane conductivity ($\Lambda = 0.4$) and along the c axis ($\Lambda = 0.06$). This is expected in the underdoped sample with larger anisotropy. From the values of the conductivities at T_c we found in the UD57 sample the coherence length $\xi_{c0} = 0.13$ nm, and the anisotropy factor $\gamma = 15$. The overall agreement of the theoretical curves with the experimental data

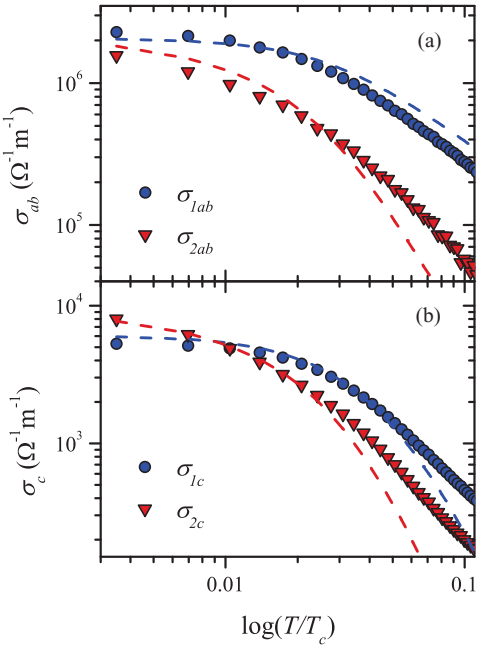

FIG. 8. (Color online) Real and imaginary parts of the complex superconducting fluctuation conductivity above T_c in deeply underdoped sample UD57. Experimental values are shown by full symbols and the dashed lines are theoretical curves as described in the text. (a) In-plane conductivity σ_{1ab} and σ_{2ab}. (b) Conductivity along the c axis σ_{1c} and σ_{2c}.

is good also in the deeply underdoped sample UD57, but it is not as remarkable as in the slightly underdoped sample UD87 shown in Fig. 7. These tests are very sensitive to the homogeneity of the sample. It is known that even a small distribution of T_c values brings about a noticeable reduction of the imaginary part σ_2 (Ref. 74). The results shown in Fig. 8 indicate that even the freshly prepared sample UD57 contained a minor distribution of T_c values, however, at this point it is not obvious whether this inhomogeneity is intrinsic to a certain doping level as has been found in $Bi_2Sr_2CaCu_2O_{8+\delta}$ (Ref. 88), and $La_{2-x}Sr_xCuO_{4+\delta}$ (Ref. 89). Regardless of its origin, this observation does not change our main conclusion in Sec. III that the superconducting fluctuations do not extend beyond 80 K, that is, they are confined within a relatively narrow region above T_c, and far below the pseudogap temperature T^* in this system. We also note that magnetization measurements in optimally doped YBCO have shown good agreement with the theoretical expectations, but a deviation appeared in a deeply underdoped sample,[65] possibly also due to some distribution of T_c values.

The superconducting fluctuations appear simultaneously in both the ab plane and along the c axis, already from the uppermost starting temperature. This observation questions some claims that, due to an increased anisotropy in underdoped samples, electronic coupling along the c axis is completely lost in this system so that only a KTB transition could take place.[90–92] Our results are also at variance with the recent microwave observations in LSCO thin films, where two-dimensional (2D) behavior was found in underdoped and in overdoped samples, while 3D behavior was established only in the optimally doped sample.[93]

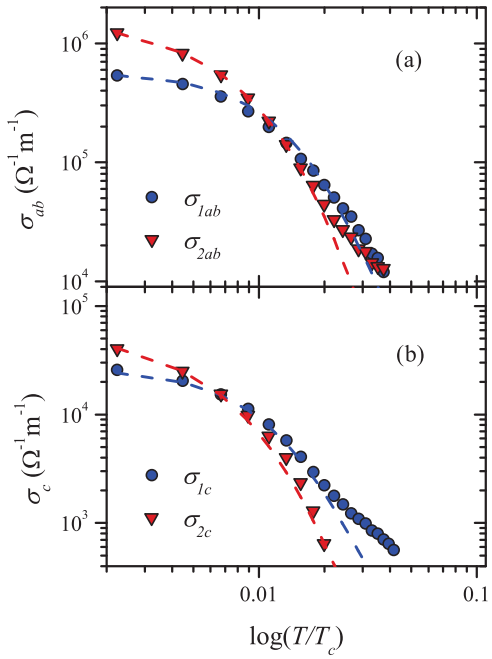

FIG. 9. (Color online) Real and imaginary parts of the complex superconducting fluctuation conductivity above T_c in overdoped sample OD89. Experimental values are shown by full symbols and the dashed lines are theoretical curves as described in the text. (a) In-plane conductivity σ_{1ab} and σ_{2ab}. (b) Conductivity along the c axis σ_{1c} and σ_{2c}.

Fluctuation conductivities have been analyzed also in our overdoped sample, and the results are shown in Fig. 9. The values of σ_{2ab} and σ_{2c} at T_c yielded parameters $\xi_{c0} = 0.17$ nm and anisotropy factor $\gamma = 5.5$. The fit parameters were $\Gamma = 0.21$ and $\Lambda = 0.026$ for the pair of fluctuation conductivities σ_{1ab} and σ_{2ab}. The fits to the pair σ_{1c} and σ_{2c} were obtained with similar values $\Gamma = 0.16$ and $\Lambda = 0.031$. The small discrepancy in the values of the crossover parameter Γ could be due to the anisotropic conductivity which occurs in the ab plane in overdoped samples, while our microwave measurement yielded an averaged value.

VI. CONCLUSION

We have presented microwave absorption measurements of YBCO single crystals in a broad doping range. By progressively increasing the applied magnetic field, we have shown that the field of 16 T is well sufficient to suppress all superconducting fluctuations above the zero field T_c. Hence, the difference of the curves measured in zero field, and in the field of 16 T is shown to be a sensitive and reliable method to detect the appearance of the superconducting fluctuations above T_c. This method does not rely on theoretical assumptions and/or models of extracting the unknown parameters from the measured data.

Our study shows that the temperature range of the superconducting fluctuations in YBCO is doping dependent. In the underdoped sample with $T_c = 57$ K, it extends at most up to 23 K above T_c. If a minor distribution of T_c values is present, the true extent of the superconducting fluctuations would appear even somewhat smaller. In any case, this relatively wide range of superconducting fluctuations is qualitatively consistent with the theoretical predictions for phase fluctuations in underdoped samples,[16–21] but provides strong evidence that the extent of the fluctuations falls well below the pseudogap temperature $T^* \approx 270$ K.

The present results, however, do not exclude the possibility of intrabilayer precursor superconducting fluctuations which might be observed by a high frequency probe, such as FIR optical conductivity measurements, at intermediate temperatures within the pseudogap region of underdoped YBCO samples.[72]

In the slightly underdoped ($T_c = 87$ K), and overdoped ($T_c = 89$ K) samples, the phase stiffness is high enough to keep the phase correlation present whenever there is some local amplitude of the order parameter. Hence, we interpret the fluctuations observed in these samples by the present method as conventional fluctuations of the complex two-component superconducting order parameter. The extent of the fluctuations is found to be 8 and 7 K in the nearly optimally doped and overdoped samples, respectively.

We have also shown that the real and imaginary parts of the fluctuation conductivity determined at our microwave frequency are in compliance with theoretical calculations which take into account the proper cutoff for the wave vector pertaining to the superconducting fluctuation modes, and renormalized behavior of the coherence length in the critical region near T_c.

ACKNOWLEDGMENTS

We would like to thank I. Kupčić, E. Tutiš, S. Barišić, A. Dubroka, C. Bernhard, and C. Berthier for numerous and invaluable discussions. This work was supported by the Croatian Ministry of Science through Grant No. 119-1191458-1022 and by the German Science Foundation under Grant No. FOR538.

*adulcic@phy.hr

[1] C. J. Lobb, Phys. Rev. B **36**, 3930 (1987).
[2] W. J. Skocpol and M. Tinkham, Rep. Prog. Phys. **38**, 1049 (1975).
[3] M. Tinkham, *Introduction to Superconductivity* (Dover Publications, New York, 2004).
[4] S. Kamal, D. A. Bonn, N. Goldenfeld, P. J. Hirschfeld, R. Liang, and W. N. Hardy, Phys. Rev. Lett. **73**, 1845 (1994).
[5] V. Pasler, P. Schweiss, C. Meingast, B. Obst, H. Wuhl, A. I. Rykov, and S. Tajima, Phys. Rev. Lett. **81**, 1094 (1998).
[6] C. Meingast, V. Pasler, P. Nagel, A. Rykov, S. Tajima, and P. Olsson, Phys. Rev. Lett. **86**, 1606 (2001).
[7] K. D. Osborn, D. J. VanHarlingen, V. Aji, N. Goldenfeld, S. Oh, and J. N. Eckstein, Phys. Rev. B **68**, 144516 (2003).
[8] S. M. Anlage, J. Mao, J. C. Booth, D. H. Wu, and J. L. Peng, Phys. Rev. B **53**, 2792 (1996).

[9]J. C. Booth, D. H. Wu, S. B. Qadri, E. F. Skelton, M. S. Osofsky, A. Piqué, and S. M. Anlage, Phys. Rev. Lett. **77**, 4438 (1996).
[10]G. Nakielski, D. Gorlitz, Chr. Stodte, M. Welters, A. Kramer, and J. Kotzler, Phys. Rev. B **55**, 6077 (1997).
[11]J. R. Waldram, D. M. Broun, D. C. Morgan, R. Ormeno, and A. Porch, Phys. Rev. B **59**, 1528 (1999).
[12]D.-N. Peligrad, M. Mehring, and A. Dulčić, Phys. Rev. B **69**, 144516 (2004).
[13]D. M. Broun, W. A. Huttema, P. J. Turner, S. Ozcan, B. Morgan, Ruixing Liang, W. N. Hardy, and D. A. Bonn, Phys. Rev. Lett. **99**, 237003 (2007).
[14]I. Hetel, T. R. Lemberger, and M. Randeria, Nat. Phys. **3**, 700 (2007).
[15]T. Timusk and B. Statt, Rep. Prog. Phys. **62**, 61 (1999).
[16]V. J. Emery and S. A. Kivelson, Nature (London) **374**, 434 (1995).
[17]V. J. Emery and S. A. Kivelson, J. Phys. Chem. Solids **59**, 1705 (1998).
[18]P. A. Lee, Physica C **317**, 194 (1999).
[19]M. Franz and Z. Tešanović, Phys. Rev. Lett. **87**, 257003 (2001).
[20]I. F. Herbut, Phys. Rev. Lett. **88**, 047006 (2002).
[21]P. W. Anderson, P. A. Lee, M. Randeria, T. M. Rice, N. Trivedi, and F. C. Zhang, J. Phys. Condens. Matter **16**, R755 (2004).
[22]C. M. Varma, Phys. Rev. B **55**, 14554 (1997).
[23]S. Chakravarty, R. B. Laughlin, Dirk K. Morr, and Chetan Nayak, Phys. Rev. B **63**, 094503 (2001).
[24]D. K. Sunko and S. Barišić, Eur. Phys. J. B **46**, 269 (2005).
[25]V. Hinkov, P. Bourges, S. Pailhès, Y. Sidis, A. Ivanov, C. D. Frost, T. G. Perring, C. T. Lin, D. P. Chen, and B. Keimer, Nature Physics **3**, 780 (2007).
[26]V. Hinkov, D. Haug, B. Fauqué, P. Bourges, Y. Sidis, A. Ivanov, C. Bernhard, C. T. Lin, and B. Keimer, Science **319**, 597 (2008).
[27]D. Haug, V. Hinkov, A. Suchaneck, D. S. Inosov, N. B. Christensen, Ch. Niedermayer, P. Bourges, Y. Sidis, J. T. Park, A. Ivanov, C. T. Lin, J. Mesot, and B. Keimer, Phys. Rev. Lett. **103**, 017001 (2009).
[28]B. Fauqué, Y. Sidis, V. Hinkov, S. Pailhès, C. T. Lin, X. Chaud, and P. Bourges, Phys. Rev. Lett. **96**, 197001 (2006).
[29]H. A. Mook, Y. Sidis, B. Fauqué, V. Balédent, and P. Bourges, Phys. Rev. B **78**, 020506 (2008).
[30]Y. Li, V. Balédent, N. Barišić, Y. Cho, B. Fauqué, Y. Sidis, G. Yu, X. Zhao, P. Bourges, and M. Greven, Nature (London) **455**, 372 (2008).
[31]J. E. Sonier, V. Pacradouni, S. A. Sabok-Sayr, W. N. Hardy, D. A. Bonn, R. Liang, and H. A. Mook, Phys. Rev. Lett. **103**, 167002 (2009).
[32]T. Kondo, R. Khasanov, T. Takeuchi, J. Schmalian, and A. Kaminski, Nature (London) **457**, 296 (2009).
[33]Z. A. Xu, N. P. Ong, Y. Wang, T. Kakeshita, and S. Uchida, Nature (London) **406**, 486 (2000).
[34]Y. Wang, L. Li, and N. P. Ong, Phys. Rev. B **73**, 024510 (2006).
[35]K. Behnia, J. Phys. Condens. Matter **21**, 113101 (2009).
[36]Olivier Cyr-Choiniere, R. Daou, Francis Laliberté, David LeBoeuf, Nicolas Doiron-Leyraud, J. Chang, J.-Q. Yan, J.-G. Cheng, J.-S. Zhou, J. B. Goodenough, S. Pyon, T. Takayama, H. Takagi, Y. Tanaka, and Louis Taillefer, Nature (London) **458**, 743 (2009).
[37]L. Li, Y. Wang, S. Komiya, S. Ono, Y. Ando, G. D. Gu, and N. P. Ong, Phys. Rev. B **81**, 054510 (2010).
[38]R. Daou, J. Chang, David LeBoeuf, Olivier Cyr-Choiniere, Francis Laliberté, Nicolas Doiron-Leyraud, B. J. Ramshaw, Ruixing Liang, D. A. Bonn, W. N. Hardy, and Louis Taillefer, Nature (London) **463**, 519 (2010).
[39]M. Ausloos and Ch. Laurent, Phys. Rev. B **37**, 611 (1988).
[40]R. Hopfengartner, B. Hensel, and G. Saemann-Ischenko, Phys. Rev. B **44**, 741 (1991).
[41]R. M. Costa, P. Pureur, L. Ghivelder, J. A. Campá, and I. Rasines, Phys. Rev. B **56**, 10836 (1997).
[42]S. H. Han, Yu. Eltsev, and O. Rapp, Phys. Rev. B **57**, 7510 (1998).
[43]K. Takenaka, K. Mizuhashi, H. Takagi, and S. Uchida, Phys. Rev. B **50**, 6534 (1994).
[44]J. Corson, R. Mallozzi, J. Orenstein, J. N. Eckstein, and I. Bozovic, Nature (London) **398**, 221 (1999).
[45]D.-N. Peligrad, M. Mehring, and A. Dulčić, Phys. Rev. B **67**, 174515 (2003).
[46]M. S. Grbić, N. Barišić, A. Dulčić, I. Kupčić, Y. Li, X. Zhao, G. Yu, M. Dressel, M. Greven, and M. Požek, Phys. Rev. B **80**, 094511 (2009).
[47]N. Barišić, Y. Li, X. Zhao, Y.-C. Cho, G. Chabot-Couture, G. Yu, and M. Greven, Phys. Rev. B **78**, 054518 (2008).
[48]V. Hinkov, S. Pailhes, P. Bourges, Y. Sidis, A. Ivanov, A. Kulakov, C. T. Lin, D. P. Chen, C. Bernhard, and B. Keimer, Nature (London) **430**, 650 (2004).
[49]J. P. Osborn, Phys. Rev. **67**, 351 (1945).
[50]J. L. Tallon, C. Bernhard, H. Shaked, R. L. Hitterman, and J. D. Jorgensen, Phys. Rev. B **51**, 12911 (1995).
[51]R. Liang, D. A. Bonn, and W. N. Hardy, Phys. Rev. B **73**, 180505(R) (2006).
[52]B. Nebendahl, D.-N. Peligrad, M. Požek, A. Dulčić, and M. Mehring, Rev. Sci. Instrum. **72**, 1876 (2001).
[53]J. Axnäs, B. Lundqvist, and Ö. Rapp, Phys. Rev. B **58**, 6628 (1998).
[54]J. Axnäs, W. Holm, Yu. Eltsev, and Ö. Rapp, Phys. Rev. Lett. **77**, 2280 (1996).
[55]W. Holm, M. Andersson, Ö. Rapp, M. A. Kulikov, and I. N. Makarenko, Phys. Rev. B **48**, 4227 (1993).
[56]V. V. Dorin, R. A. Klemm, A. A. Varlamov, A. I. Buzdin, and D. V. Livanov, Phys. Rev. B **48**, 12951 (1993).
[57]I. Ukrainczyk and A. Dulčić, Phys. Rev. B **51**, 6788 (1995).
[58]J. I. Gittleman and B. Rosenblum, Phys. Rev. Lett. **16**, 734 (1966).
[59]M. W. Coffey and J. R. Clem, Phys. Rev. Lett. **67**, 386 (1991).
[60]A. Dulčić and M. Požek, Physica C **218**, 449 (1993).
[61]Y. Ando, S. Komiya, K. Segawa, S. Ono, and Y. Kurita, Phys. Rev. Lett. **93**, 267001 (2004).
[62]Y. Ando and K. Segawa, Phys. Rev. Lett. **88**, 167005 (2002).
[63]M. Požek, M. S. Grbić, N. Barišić, and A. Dulčić, unpublished results.
[64]N. Bergeal, J. Lesueur, M. Aprili, G. Faini, J. P. Contour, and B. Leridon, Nature Physics **4**, 608 (2008).
[65]P. Carretta, A. Lascialfari, A. Rigamonti, A. Rosso, and A. Varlamov, Phys. Rev. B **61**, 12420 (2000).
[66]F. Rullier-Albenque, R. Tourbot, H. Alloul, P. Lejay, D. Colson, and A. Forget, Phys. Rev. Lett **96**, 067002 (2006).
[67]David LeBoeuf, Nicolas Doiron-Leyraud, Julien Levalolois, R. Daou, J.-B. Bonnemaison, N. E. Hussey, L. Balicas, B. J. Ramshaw, Ruixing Liang, D. A. Bonn, W. N. Hardy, S. Adachi, Cyril Proust, and Louis Taillefer, Nature (London) **450**, 533 (2007).
[68]C. C. Homes, S. V. Dordevic, D. A. Bonn, Ruixing Liang, W. N. Hardy, and T. Timusk, Phys. Rev. B **71**, 184515 (2005).

[69]N. E. Hussey, M. Abdel-Jawad, A. Carrington, A. P. Mackenzie, and L. Balicas, Nature (London) **425**, 814 (2003).
[70]J. Lee, K. Fujita, A. R. Schmidt, C. K. Kim, H. Eisaki, S. Uschida, and J. C. Davis, Science **325**, 1099 (2009).
[71]L. Yu, D. Munzar, A. V. Boris, P. Yordanov, J. Chaloupka, Th. Wolf, C. T. Lin, B. Keimer, and C. Bernhard, Phys. Rev. Lett. **100**, 177004 (2008).
[72]A. Dubroka, M. Rössle, K. W. Kim, V. K. Malik, D. Munzar, D. N. Basov, A. Schafgans, S. J. Moon, C. T. Lin, D. Haug, V. Hinkov, B. Keimer, Th. Wolf, J. G. Storey, J. L. Tallon, and C. Bernhard, Phys. Rev. Lett. **106**, 047006 (2011).
[73]I. Ussishkin, S. L. Sondhi, and David A. Huse, Phys. Rev. Lett. **89**, 287001 (2002).
[74]H. Kitano, T. Ohashi, A. Maeda, and I. Tsukada, Phys. Rev. B **73**, 092504 (2006).
[75]L. S. Bilbro, R. V. Aguilar, G. Logenov, I. Bozovic, and N. P. Armitage, Nature Physics (2011), doi:10.1038/nphys1912.
[76]N. E. Hussey, H. Takagi, Y. Iye, S. Tajima, A. I. Rykov, and K. Yoshida, Phys. Rev. B **61**, R6475 (2000).
[77]H. Kitano, T. Shibauchi, K. Uchinokura, A. Maeda, H. Asaoka, and H. Takei, Phys. Rev. B **51**, 1401 (1995).
[78]H. Schmidt, Z. Phys. **216**, 336 (1968).
[79]A. T. Dorsey, Phys. Rev. B **43**, 7575 (1991).
[80]R. A. Wickham and A. T. Dorsey, Phys. Rev. B **61**, 6945 (2000).
[81]B. R. Patton, V. Ambegaokar, and. J. W. Wilkins, Solid State Commun. **7**, 1287 (1969).
[82]J. P. Gollub, M. R. Beasley, R. Callarotti, and M. Tinkham, Phys. Rev. B **7**, 3039 (1973).
[83]E. Silva, Eur. Phys. J. B **27**, 497 (2002).
[84]E. Silva, R. Marcon, S. Sarti, R. Fastampa, M. Giura, M. Boffa, and A. M. Cuccolo, Eur. Phys. J. B **37**, 277 (2004).
[85]V. Aji and N. Goldenfeld, Phys. Rev. Lett. **87**, 197003 (2001).
[86]H. Xu, S. Li, S. M. Anlage, C. J. Lobb, M. C. Sullivan, K. Segawa, and Y. Ando, Phys. Rev. B **80**, 104518 (2009).
[87]D. Neri, E. Silva, S. Sarti, R. Marcon, M. Giura, R. Fastampa, and N. Sparvieri, Phys. Rev. B **58**, 14581 (1998).
[88]K. K. Gomes, A. N. Pasupathy, A. Pushp, S. Ono, Y. Ando, and A. Yazdani, Nature (London) **447**, 569 (2007).
[89]I. Iguchi, T. Yamaguchi, and A. Sugimoto, Nature (London) **412**, 420 (2001).
[90]L. B. Ioffe and A. J. Millis, J. Phys. Chem. Solids **63**, 2259 (2002).
[91]I. F. Herbut and M. J. Case, Phys. Rev. B **70**, 094516 (2004).
[92]F. Rullier-Albenque, H. Alloul, Cyril Proust, P. Lejay, A. Forget, and D. Colson, Phys. Rev. Lett. **99**, 027003 (2007).
[93]T. Ohashi, H. Kitano, I. Tsukada, and A. Maeda, Phys. Rev. B **79**, 184507 (2009).